Optimizing the Radar Detection of Clear Air Turbulence[1]

DAVID ATLAS[2] AND KENNETH R. HARDY
Air Force Cambridge Research Laboratories, Sudbury, Mass.
AND KEIKICHI NAITO[3]
Northeastern University, Boston, Mass.

(Manuscript received 4 February 1966, in revised form 6 April 1966)

ABSTRACT

A general analysis is made of the turbulent refractivity spectrum in and beyond the limiting microscale and a relation derived for its scattering reflectivity in either the back or bistatic directions. Radar reflectivity is computed as a function of wavelength for regions of CAT. The results are compared to the minimum detectable reflectivity of airborne radars having optimum state of the art characteristics at each wavelength. It is shown that the best radars now feasible can barely detect the most reflective CAT at 10 n mi (i.e., 1 minute warning). A 20-db improvement in sensitivity is required for detection of most CAT, which appears to be just attainable by pre-detection integration. The optimum wavelength to implement is 5–6 cm. The best radar at this wavelength will also detect cirrus clouds reliably. Whether detecting clouds or chaff a measure of the echo fluctuation (or Doppler) spectrum is required to identify the intensity of CAT. However, in the case of high altitude clear air echoes, there is an indication that the reflectivity in excess of some minimum threshold value is a sign of some degree of mechanical turbulence. It is also demonstrated that a ground-based forward-scatter link holds great promise for reliable CAT detection. A tentative quantitative classification of CAT severity is also proposed.

1. Introduction

In general, vertical velocity perturbations in an atmosphere having a vertical gradient of refractivity will introduce perturbations in refractivity. If the magnitude of such refractivity perturbations is sufficiently large at a scale corresponding to half the wavelength of a radar, then the radar may detect the perturbed region. Thus, the objectives of this paper are to determine: 1) the magnitude and spectrum of the refractivity perturbations likely to exist in regions of clear air turbulence (CAT); 2) the magnitude and wavelength dependence of the signals scattered from such regions; and 3) the optimum wavelength for detecting CAT in consideration of the state of the art variation of overall system sensitivity with wavelength. Consideration will also be given to the possibility of detecting CAT by forward-scatter techniques.

Smith and Rogers (1963) undertook a preliminary study of some of these questions. However, they lacked a quantitative estimate of the refractivity spectrum at small scales and so were unable to calculate the backscatter at short wavelengths. Moreover, they failed to consider the variations in attainable radar system sensitivity as a function of wavelength, and so could not deduce the optimum wavelength for CAT detection. These short-comings are overcome in the present paper. It should also be noted that our treatment is applicable generally to problems of electromagnetic scatter from turbulent media.

2. Theory

The one-dimensional power spectrum of turbulence. Employing the generally accepted equilibrium theory of isotropic homogeneous turbulence (Obukhov, 1949), we may express the one-dimensional energy spectrum of the velocity perturbations by

$$E(k)=A_1\epsilon^{2/3}k^{-5/3}, \tag{1a}$$

where ϵ (cm^2 sec^{-3}) is the rate of dissipation of turbulent energy per unit mass, k (cm^{-1}) is the wave number corresponding to the scale $L=2\pi/k$, and A_1 is a constant whose value, based on both theory and experiment, is 0.5 for perturbations along the direction of flow and 0.64 for those transverse to the flow (Panofsky and Pasquill, 1963). These coefficients apply only when the wave number is expressed in radians per unit length. $E(k)$ is the Fourier transform of the space correlation function of velocity perturbations, and so $E(k)dk$ is the

[1] This research has been partially supported by the Air Force In-House Laboratory Independent Research Fund. A preliminary version of this paper appears in the Proceedings of the Clear Air Turbulence Meeting, 23–24 February 1966, Washington, D. C., Institute of Navigation and Society of Automotive Engineers, 97–106.

[2] Present affiliation: Department of Geophysical Sciences, University of Chicago.
[3] On leave from the Meteorological Research Institute, Tokyo, Japan.

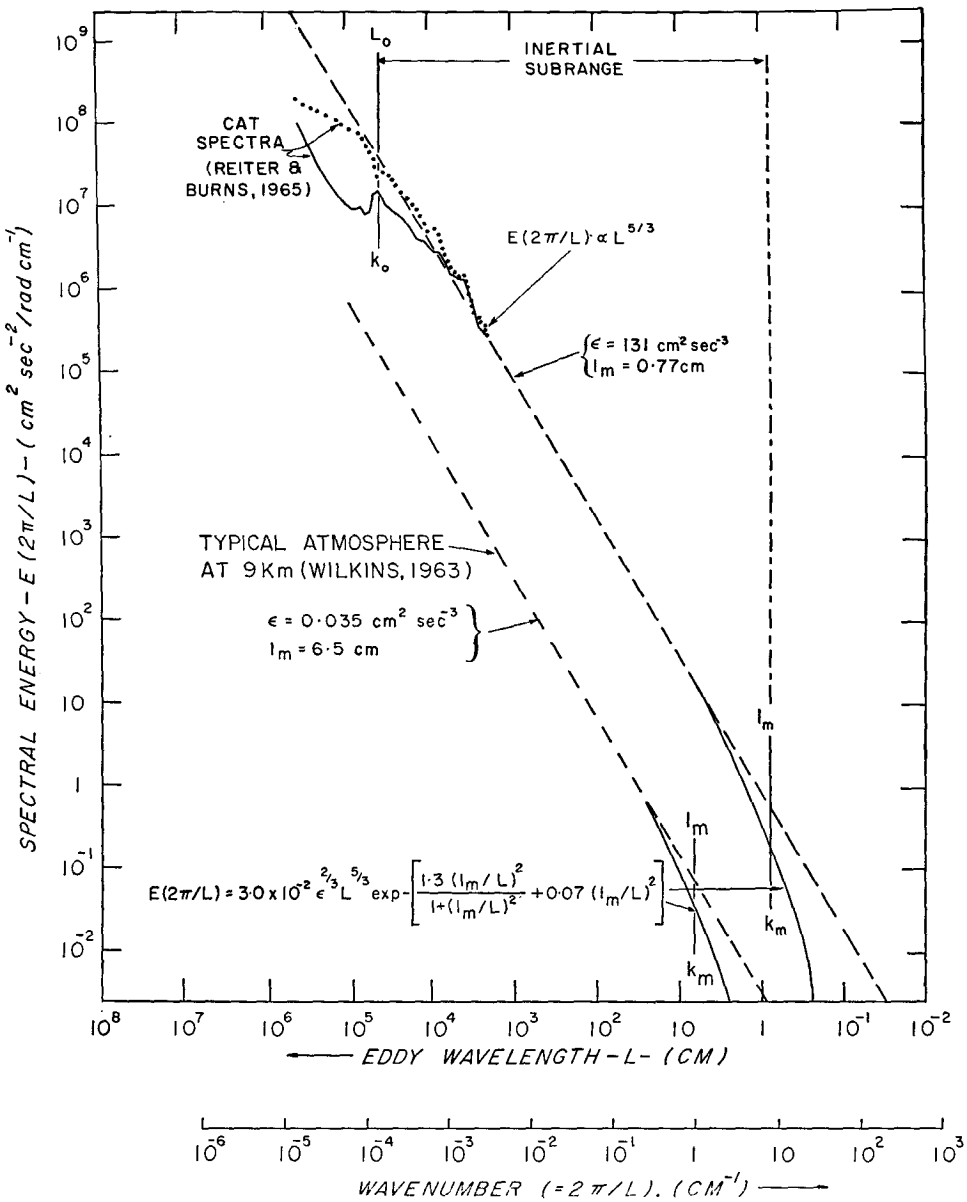

FIG. 1. The spectrum of $E(k)$ typical of CAT regions (upper curve) and of the quiet atmosphere at 9 km (lower curve). The spectrum in the region of the limiting microscale is obtained from Gurvitch *et al.* (1965). Two spectra measured with an aircraft in CAT are shown at the upper left.

contribution to the velocity variance by eddies of wave number k to $k+dk$. Since kinetic energy is $\frac{1}{2}m(v')^2$, where v' is the velocity perturbation, $E(k)dk$ is actually twice the kinetic energy per unit mass of air. If the velocity field is isotropic then the total kinetic energy per unit mass in all three dimensions is $(3/2)\int_0^\infty E(k)dk$. Using $A_1=0.64$, $k=2\pi/L$, we obtain

$$\epsilon=192[E(k)]^{\frac{3}{2}}L^{-\frac{5}{2}}. \tag{1b}$$

Eq. (1) is valid over the so-called inertial subrange $k_0<k<k_m$, where $k_0=2\pi/L_0$, $k_m=2\pi/\ell_m$, L_0 is the outer scale and ℓ_m is the limiting microscale. Both of these limits are of interest throughout this work.

In order to estimate ℓ_m from radar reflectivity or forward-scatter measurements, we must know how the spectral density of velocity (or refractivity) fluctuations varies beyond the small-scale limit of the inertial subrange. Gurvitch *et al.* (1965) quote the results of Gorshkov[4] who suggests an approximation to the one-dimensional spectrum of longitudinal velocity fluctuations near the microscale based on recent empirical data, of the form

$$\gamma(X)=\exp[-(1.3X^2)/(1+X^2)-0.07X^2], \tag{2}$$

[4] N. F. Gorshkov, Institute of Atmospheric Physics, Moscow.

where $\chi=k/k_m$, the wave number normalized with respect to that at the limiting microscale of the inertial subrange. In contrast to the assumed seventh power law which has been used in the past to describe the shape of the spectrum for very small eddies (MacCready, 1962), the exponential forms given by Eq. (2) and by Pao (1964) show good agreement with the observations obtained so far.

Using Eq. (2) we may write the one-dimensional energy spectrum [Eq. (1a)] as

$$E(k)=A_1\epsilon^{2/3}k^{-5/3}\gamma(\chi), \tag{3}$$

an equation which is now valid $k>k_0$ or $L<L_0$. The spectrum $E(k)$ for a value of ϵ and ℓ_m typical of CAT regions is shown as the upper curve of Fig. 1. The limits of the inertial subrange are indicated by L_0 and ℓ_m. The lower curve of Fig. 1 represents a spectrum of the typical quiet atmosphere at 9 km which was computed using a value of $\epsilon=0.035$ cm^2 sec^{-3} given by Wilkins (1963). Note that the energy in CAT is more than two orders of magnitude larger than that which is estimated for the normally non-turbulent atmosphere. Some spectra measured with an aircraft in CAT by Reiter and Burns (1965) are also shown at the upper left of Fig. 1. It is clear that only a small fraction of the inertial subrange can be obtained from aircraft measurements. The energy spectrum near the limiting microscale must be measured with extremely fast response instruments which are normally held stationary near the earth's surface (Gurvitch *et al.*, 1965). Once a region of the spectrum is established with the $k^{-5/3}$ dependence, it is reasonable to extrapolate down to $k\sim k_m$, corresponding to the microscale, for this is in accord both with theory and experiment. However, it is not as valid to extrapolate the spectrum in the other direction to the outer scale L_0 since this limit depends upon the mesoscale structure of the atmosphere. Fortunately, in the case of CAT we now have some reasonable measurements of L_0.

The outer scale is defined by

$$L_0=(\kappa/\beta)^{\frac{1}{2}}, \tag{4}$$

where κ is the coefficient of eddy diffusivity and $\beta=d\bar{u}/dz$, the vertical gradient of the mean horizontal wind (Tatarski, 1961). On the other hand ϵ is related to these quantities by

$$\epsilon=\kappa\beta^2. \tag{5}$$

Substituting into Eq. (4) we have

$$L_0=(\epsilon/\beta^3)^{\frac{1}{2}}. \tag{6}$$

Thus, the outer scale is related to the vertical gradient of the mean wind and the rate of energy dissipation.

Let us now consider how the limiting microscale is related to turbulent kinetic energy. Megaw (1957) defines ℓ_m by

$$\ell_m=5.9(\nu^3/\epsilon)^{\frac{1}{4}}, \tag{7a}$$

where ν is the coefficient of kinematic viscosity. Since ν varies only slightly with altitude, we take $\nu=0.335$ cm^2 sec^{-1} corresponding to an altitude of about 9 km and a temperature of -35C. Thus

$$\ell_m\sim 2.6\epsilon^{-\frac{1}{4}} \tag{7b}$$

for the pertinent regions of CAT. Now since the kinetic energy $E(k)\propto\epsilon^{2/3}$ [Eq. (1a)], we find also that $E(k)\propto\ell_m^{-8/3}$. In other words, the limiting microscale is a function of the turbulent energy; the greater the turbulence, the smaller ℓ_m (Fig. 1). Clearly, if we could measure either ϵ or ℓ_m, we would have an approximate measure of the intensity of turbulence.

Reflectivity of a turbulent medium. Tatarski and others have shown that the reflectivity (cross section per unit volume) of a refractively turbulent medium is given by

$$\eta=\pi\sin^2\beta\,\overline{(\Delta n)^2}k^2F_n(k)[8\sin^4(\theta/2)]^{-1}, \tag{8}$$

where θ is the angle between the transmitter and receiver beams, β is the angle between the direction of the receiver and that of the electric field of the incident wave, $k=(4\pi/\lambda)\sin(\theta/2)$, λ is the wavelength of the incident radiation, $\overline{(\Delta n)^2}$ is the mean square fluctuation in refractivity and $F_n(k)$ is the one-dimensional spectral density of $(\Delta n)^2$ in terms of wave number. Strictly speaking, $F_n(k)$ is the Fourier transform of the space autocorrelation function of n. (If the field of n is not isotropic then $F_n(k)$ is the Fourier spectrum of n along a direction perpendicular to the bisector between the directions of transmission and reception (i.e., along the line of sight for radar back scatter, and along the vertical for a forward-scatter link). While the spectrum $F_n(k)$ may extend over a great range, the reflectivity is determined only by the spectral density at wave number $k=(4\pi/\lambda)\sin(\theta/2)$ or scale $L=\lambda/[2\sin(\theta/2)]$. In the radar case, of course, the scale of interest is precisely $\lambda/2$.

In a manner analogous to Eq. (1a), the one-dimensional spectrum of refractivity may be expressed (Tatarski, 1961) as

$$F_n(k)=\tfrac{2}{3}k_0^{2/3}k^{-5/3}, \tag{9}$$

which is valid in the inertial subrange. Normalizing with respect to the wave number of the limiting microscale k_m and multiplying by the empirical expression (2) to extend (9) into the region of $k>k_m$, we find

$$F_n(\chi)=\tfrac{2}{3}\chi_0^{2/3}\chi^{5/3}\gamma(\chi), \tag{10}$$

where $\chi=k/k_m$, $\chi_0=k_0/k_m$ and $F_n(k)=F_n(\chi)/k_m$. Eq. (10) is now valid for all $\chi>\chi_0$ or $L<L_0$. Substituting (10) into (8), we obtain the general expression

$$\eta=(\pi/12)\sin^2\beta\,\overline{(\Delta n)^2}k_m\chi_0^{\frac{2}{3}}\chi^{\frac{1}{3}}\gamma(\chi)/\sin^4(\theta/2). \tag{11}$$

In the back-scatter direction $\beta=\pi/2$, $\theta=\pi$ and $\chi=2\ell_m/\lambda$, so that the normalized radar reflectivity becomes

$$\eta\ell_m^{\frac{1}{3}}=2.1\,\overline{(\Delta n)^2}L_0^{-\frac{2}{3}}(\chi/2)^{\frac{1}{3}}\gamma(\chi). \tag{12}$$

It may also be shown (Hardy *et al.*, 1966) that

$$\overline{(\Delta n)^2}=0.19L_0^{\frac{2}{3}}C_n^2, \tag{13}$$

where C_n^2 is a measure of the intensity of refractivity fluctuations as expressed by the coefficient employed by Tatarski (1961) in the three-dimensional refractivity spectrum. Substituting (13) into (12) we obtain

$$\eta\ell_m^{\frac{1}{3}}=0.39C_n^2(\chi/2)^{\frac{1}{3}}\gamma(\chi). \tag{14}$$

Eqs. (11), (12) and (14) are valid for $\chi>\chi_0$ or for $L<L_0$.

The quantity $\eta\ell_m^{\frac{1}{3}}/C_n^2$ (the reflectivity normalized for both the limiting microscale and the coefficient C_n^2) is plotted in Fig. 2 versus λ/ℓ_m. We see immediately that the reflectivity is peaked at $\lambda=5\ell_m$ and that the $\lambda^{-\frac{1}{3}}$ law (as predicted for the inertial subrange and used by Smith and Rogers, 1963) is applicable only at $\lambda\gtrsim 10\ell_m$.

3. The reflectivity of CAT regions

In order to make a realistic estimate of the reflectivity and its wavelength dependence in regions of CAT, we must estimate both C_n^2 and ℓ_m, the limiting microscale, for use in Eq. (14). Tatarski (1961) gives

$$C_n^2=a^2L_0^{4/3}M^2, \tag{15}$$

where a^2 is a non-dimensional proportionality parameter and $M=\overline{(dn/dz)}$, the mean vertical gradient of potential refractivity. The following values of the parameters in Eq. (15) are suggested for regions of CAT:

$a^2=2$, corresponding to a Richardson number of 0.05 (Tatarski, 1960),

$L_0=100$–600 m, based on CAT spectra of Reiter and Burns (1965) and Vinnichenko *et al.* (1965),

$M=4.4\times10^{-11}$ cm^{-1}, obtained from the equation

$$M=-79\times10^{-6}pT^{-2}d\theta/dz, \tag{16}$$

where p and T are the mean pressure (mb) and absolute temperature, respectively, and θ is the potential temperature. At 9 km, $p\sim300$ mb, $T\sim233$K. Assuming that CAT occurs preferentially in thermally stable layers (Panofsky, 1965), we take $d\theta/dz=10^{-4}$ (°K) cm^{-1} corresponding to an isothermal region. (The lapse in the standard atmosphere is only 60 per cent smaller). On this basis we find that C_n^2 ranges from about 10^{-15} to 10^{-14} cm$^{-\frac{2}{3}}$ over the indicated range of L_0. Assuming somewhat smaller values of both L_0 and $d\theta/dz$, a lower limit of C_n^2 is about 10^{-16} cm$^{-\frac{2}{3}}$. Thus, for CAT, a reasonable range of C_n^2 appears to be 10^{-16} to 10^{-14} cm$^{-\frac{2}{3}}$. To the extent that both C_n^2 and σ_v^2, the velocity variance of the turbulence spectrum (Eq. 17), are increasing functions of L_0, then C_n^2 and the reflectivity are related to the intensity of mechanical turbulence. Indeed, at high altitudes where M, the vertical refractivity gradient, is limited in magnitude, we may find that values of $C_n^2\gtrsim10^{-15}$ cm$^{-\frac{2}{3}}$ imply sufficiently large values of L_0 to be associated with significant mechanical turbulence (see Supplementary note, Section 7).

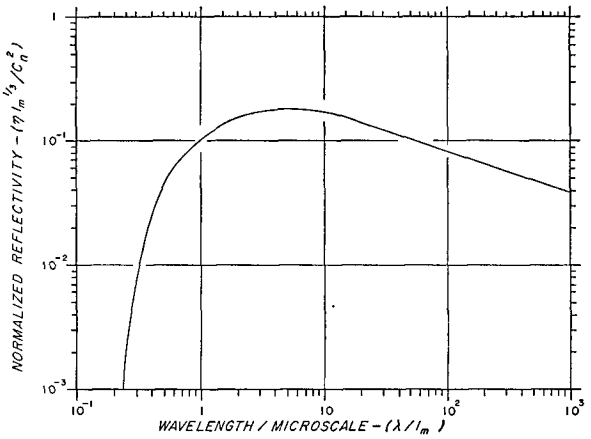

FIG. 2. Normalized clear-air reflectivity versus wavelength/microscale ratio.

It will be noted that Eq. (16) omits any consideration of the contribution of moisture to the refractivity. This is reasonable at the altitudes with which we are concerned since the moisture term contributes only a few per cent to the refractivity even under saturated conditions at $p=300$ mb and $T=233$K.

It may appear paradoxical that CAT should occur in or near thermally stable zones which are usually associated with non-turbulent conditions. However, it is at such stable strata that strong shear can develop and produce sufficiently small Richardson numbers to cause turbulent breakdown. The resulting patch of turbulence is thought to move off downstream and ultimately dissipate. In the turbulent region, the shear is diminished or destroyed, but the large scale atmospheric processes work to re-establish it.

Now consider the limiting microscale ℓ_m, related to ϵ through Eq. (7b), and plotted in Fig. 3. In a stable non-turbulent atmosphere, ϵ decreases rapidly with height to a value of $\epsilon\sim4\times10^{-2}$ cm^2 sec^{-3} at 9 or 10 km (Wilkins, 1963). However, in CAT regions ϵ may be as large as 10^3 cm^2 sec^{-3} (Panofsky, 1965). To estimate ϵ in CAT, we have employed the energy spectra of Reiter and Burns (1965) and Vinnichenko *et al.* (1965) thus obtaining values of $E(k)$ for use in Eq. (1b). Both of these studies show that the $-5/3$ law is applicable in CAT for scales smaller than about 600 m, which is a reasonable estimate of the outer scale. Moreover, Reiter and Burns (1965) show that the turbulence is approximately isotropic. Thus, we may take the values of $E(k)$ at a scale $L=10^2$ m ($k=2\pi\times10^{-4}$ cm^{-1}) as a measure of ϵ. This will be written as E_{100}. At $L=10^2$ m, Eq. (1a) gives $E_{100}=1.4\times10^5\,\epsilon^{\frac{2}{3}}$ where E_{100} is in cgs units[5] of cm^2 sec^{-2} rad^{-1} cm and ϵ is in cm^2 sec^{-3}.

[5] Reiter and Burns (1965) give $E(k)$ in units of ft^2 sec^{-2} cycle^{-1} ft; to convert to cm^2 sec^{-2} rad^{-1} cm, multiply by 4.52×10^3. Vinnichenko *et al.* (1965) give $E(k)$ in units of km^2 hr^{-2} rad^{-1} km; to convert to cm^2 sec^{-2} rad^{-1} cm, multiply by 7.73×10^7.

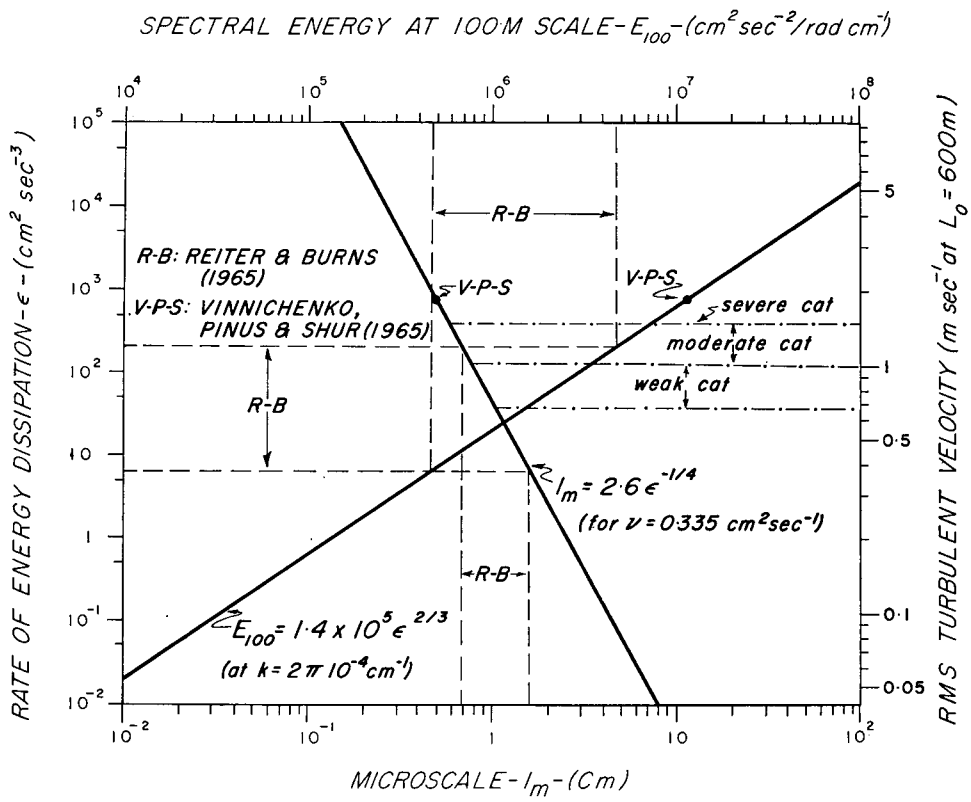

FIG. 3. Relationship between the microscale (ℓ_m), the spectral energy at 100 m scale (E_{100}), the rms turbulent velocity (σ_v), and the rate of energy dissipation (ϵ). Observed limits of E_{100} in CAT are indicated by the dashed lines. CAT intensity classes are tentative.

The relation between E_{100} and ϵ is also plotted in Fig. 3.

From the data of Reiter and Burns we find E_{100} ranges from about 4.5×10^5 to 4.5×10^6 cm^2 sec^{-2} rad^{-1} cm for CAT of intensity ranging from light to severe, thus giving ϵ values ranging between 6 and 200 cm^2 sec^{-3} and corresponding microscale ℓ_m between 1.5 and 0.7 cm, respectively, as shown in Fig. 3. From one case of severe CAT reported by Vinnichenko *et al.* (1965) at a height of 8 km, we find $E_{100}=1.2\times10^7$ cm^2 sec^{-2} rad^{-1} cm and $\epsilon=760$ cm^2 sec^{-3}. In Fig. 3 we see that this falls above the largest values reported by Reiter and Burns. The designation of the severity of CAT is presently subjective; moreover, it depends upon the type of aircraft employed and its speed. Nevertheless, with the information available it is possible to arrive at a tentative classification of CAT intensities. Such a classification is indicated in Fig. 3 and Table 1. This classification is based on the following qualitative guide lines: 1) a value of $\epsilon\sim50$ cm^2 sec^{-3} is roughly the lower limit below which Gorelik *et al.* (1963) indicate an aircraft does not experience noticeable turbulence, and 2) the threshold of severe CAT should not fall too far above the larger values of E reported by Reiter and Burns but should fall below the severe report of Vinnichenko *et al.* The parameter $R=(\epsilon\rho/\rho_0)^{\frac{1}{3}}$, where ρ is the air density at the level of CAT and ρ_0 the air density at sea level, has been proposed by MacCready *et al.* (1965) as a universal turbulence number. Their four categories for R are light (R=0.8–1.9), moderate (1.9–4.5), heavy (4.5–10.7) and severe (>10.7) in units of cm$^{\frac{1}{3}}$ sec^{-1}. While these values are in general accord with our classification in the mid-range, they extend to greater extremes of light and severe turbulence. The use of four categories instead of three will have to be justified by experience. In any case, it is interesting to note the general agreement between the two independently derived classification schemes.

TABLE 1. Spectral parameters versus CAT severity.

Parameter	CAT severity Weak		Moderate		Severe
E_{100} (cm^3 sec^{-2})	1.5×10^6	<	3.2×10^6	<	7×10^6
ϵ (cm^2 sec^{-3})	35	<	110	<	400
ℓ_m (cm)	1.0	>	0.8	>	0.6
σ_v (m sec^{-1})	0.67	<	1.0	<	1.5
$R[=(\epsilon\rho/\rho_0)^{\frac{1}{3}}]$ (cm$^{\frac{1}{3}}$ sec^{-1})	2.4	<	3.5	<	5.3

In order to obtain an estimate of the meaning of the above ϵ and E_{100} values in terms of the rms turbulent velocity, we may integrate Eq. (1a) over the inertial subrange to obtain the velocity variance σ_v^2. If $L_0\geq10^3\ell_m$

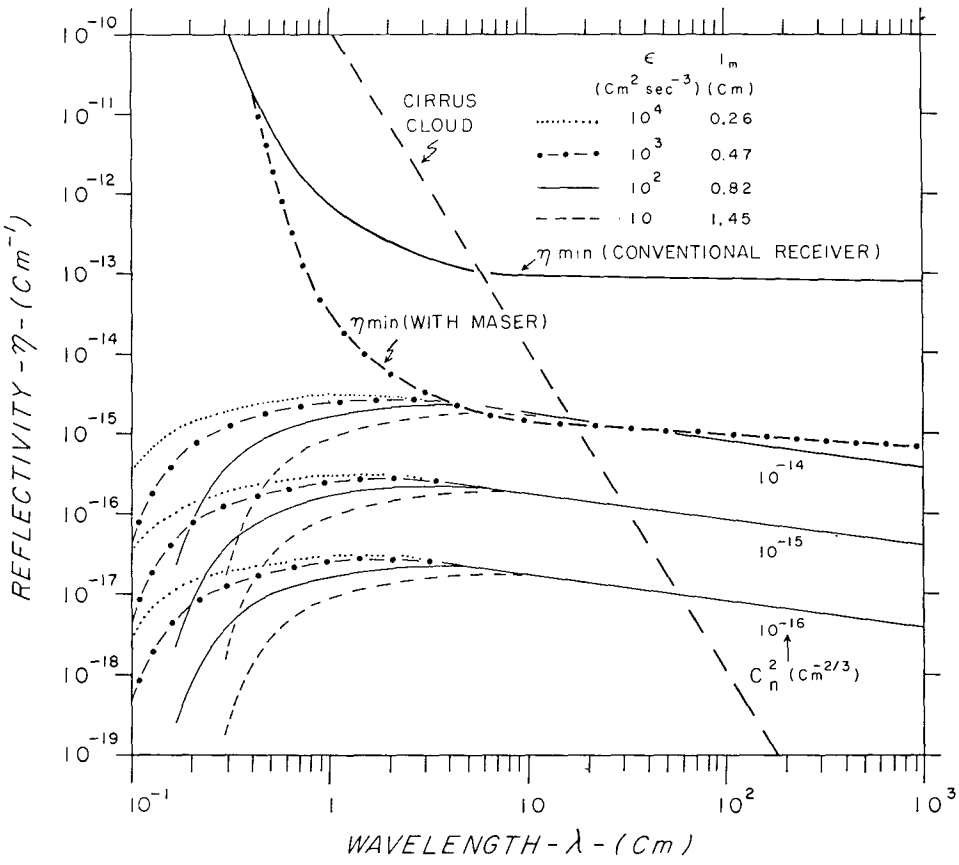

FIG. 4. Curves of clear air reflectivity for various microscales (ℓ_m) or dissipation rates (ϵ) and C_n^2 values expected in CAT are shown in the lower half of the figure. The straight dashed line is the reflectivity of a typical cirrus cloud. The curves of minimum detectable reflectivities for optimum airborne radars shown in the upper half of the figure are discussed in Section 4.

(or $k_m \geq 10^3 k_0$), then it is found that

$$\sigma_v^2 = \tfrac{3}{2} A_1 \epsilon^{\frac{2}{3}} k_0^{-\frac{2}{3}} \tag{17}$$

to better than 1 per cent accuracy. Assuming $L_0 = 600$ m for CAT and $A_1 = 0.64$, then

$$\sigma_v = 20.5 \epsilon^{\frac{1}{3}}. \tag{18}$$

The σ_v values of Table 1 and on the right ordinate of Fig. 3 are based on this relationship. In other words, our tentative classification suggests that rms velocity perturbations of 0.67, 1.0 and 1.5 m sec^{-1} correspond to the thresholds of weak, moderate and severe CAT, respectively. As a matter of fact we used these values of σ_v, which are easily remembered, to determine the precise bounds of ϵ and E for the various categories. Thus, while the general classification proposed has empirical support, the exact limits are somewhat arbitrary. We emphasize that the classification is still tentative.

Having estimated the ranges of C_n^2 and ℓ_m, we may now use Eq. (14) to calculate the reflectivity-wavelength dependence for CAT. This is shown in Fig. 4 using C_n^2 and ℓ_m as parameters. At $\lambda \lesssim 5$ cm, reflectivity is a function of both ℓ_m and C_n^2. Thus, at short wavelengths we find a family of curves for each C_n^2, each one of the family corresponding to a different ℓ_m, according to the legend. Thus, measurements of reflectivity at two or more wavelengths in the short wave regions would identify the value of ℓ_m. Since ℓ_m is a unique function of ϵ [Eq. (7a)], in principle at least, we would then have a measure of the intensity of turbulence. Unfortunately, however, we shall find that detection at the shorter wavelengths is not feasible. On the other hand, at $\lambda \gtrsim 5$ cm where η is a function only of C_n^2, the reflectivity is indicative of mechanical turbulence only to the extent that C_n^2 is dependent upon L_0, the outer scale of the turbulence spectrum [Eq. (15)]. Incidentally, the straight dashed line in Fig. 4 is the reflectivity of a typical cirrostratus cloud (i.e., $\eta \propto \lambda^{-4}$). Also the two curves in the upper half of Fig. 4 represent the minimum detectable reflectivities under the conditions discussed in the next section.

4. Minimum detectable reflectivity

Now, in order to select an optimum wavelength for CAT detection, we must first estimate the maximum attainable system sensitivity as a function of wave length.

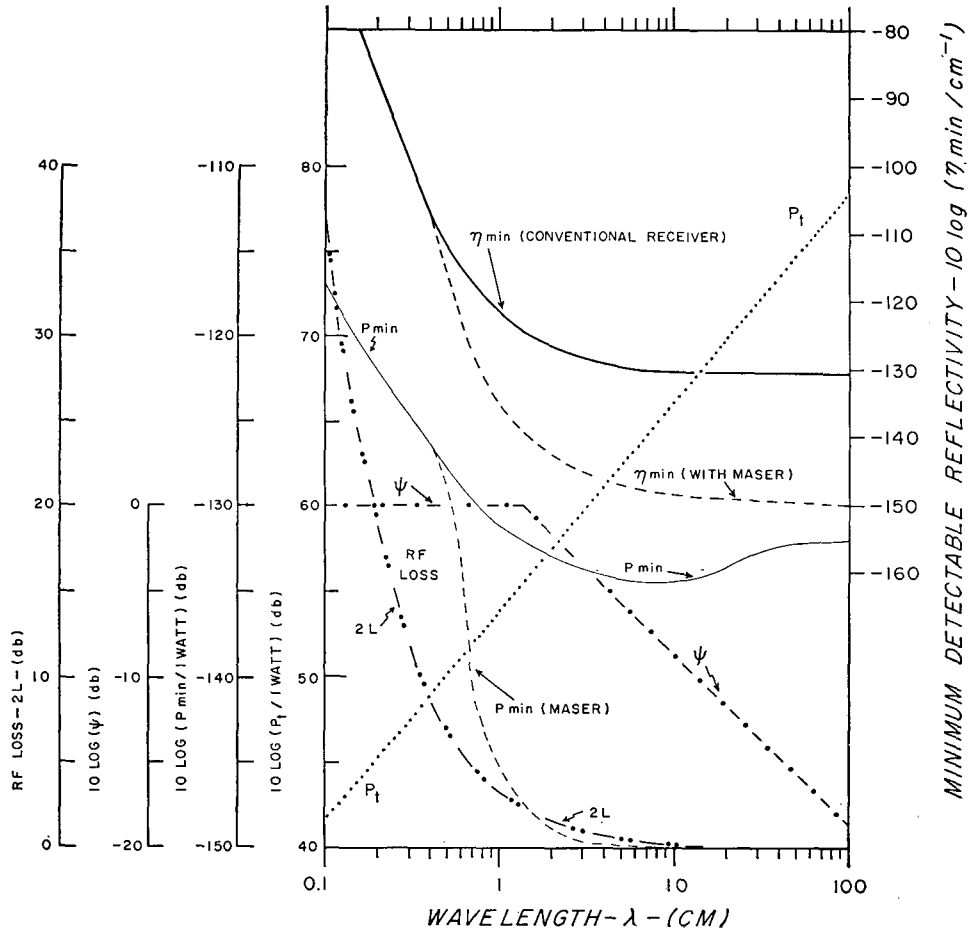

FIG. 5. Best state of the art values of the parameters of an airborne radar as a function of wavelength and corresponding minimum detectable reflectivities at 10 n mi range. See text for details.

Employing the radar equation for distributed targets (Atlas, 1964), the minimum detectable reflectivity may be written as

$$\eta_{\min}=P_{\min}8\pi r^2/(0.445P_t\psi A_e h10^{-2L}), \qquad (19)$$

where $P_{\min}=NKTB$, N is the receiver noise figure, $K=1.38\times10^{-16}$ ergs (°K)$^{-1}$, T is the receiver noise temperature, B the receiver band width, P_t the peak transmitter power, A_e the effective antenna aperture, ψ the fraction of the beam filled and L the losses in waveguide and RF components in decibels. Strictly speaking, $\eta_{\min}$ is the single pulse detectability of an echo having an intensity equal to the average from the scattering volume. Obviously, Eq. (19) is optimistic in that the probability of discerning a signal equal to the noise power with confidence is small. Nevertheless, it provides a useful limiting estimate of the radar capability.

We consider an airborne radar providing a 1-min warning of CAT at aircraft speeds of 600 kt, i.e., detection range r must be 10 n mi (18.5 km). The size of a practical airborne antenna is limited to about 1 m diameter; thus, at 67 per cent efficiency $A_e=5.23\times10^3$ cm^2. We choose a 1-μsec pulse ($h=300$ m) since it is believed that some Doppler differential measurements between adjacent pulse volumes will ultimately be required in order to characterize the scattering region as turbulent. With these factors as constant, we then have

$$\eta_{\min}=1.22\times10^6P_{\min}/(P_t\psi10^{-0.2L}). \qquad (20)$$

In order to estimate the beam filling factor ψ, we consider a turbulent layer 250 m deep extending uniformly to fill even the largest beam in a horizontal direction at a range of 18.5 km. The vertical angle subtended by this layer is 1.36×10^{-2} radians. The vertical beam width of an antenna of 100 cm diameter is $\lambda/D=10^{-2}\lambda$ radians. Thus, the fraction of the beam filled is given approximately as $\psi=1.36/\lambda$ at $\lambda>1.36$ cm; $\psi=1$ at $\lambda\leq1.36$ cm.

We now attempt to estimate the wavelength dependence of the minimum receiver sensitivity ($P_{\min}$), the maximum peak transmitted power (P_t) and minimum RF losses (L) permitted by the state of the art. These estimates, shown in Fig. 5, were made with the

aid of a recent paper by O'Kelley[6] based on surveys by Sylvania,[7] Dees and Sheppard (1963) and Nichols *et al.* (1964). The RF losses shown in Fig. 5 correspond to the two way losses through 4 ft of waveguide (O'Kelley[6]). While it may be possible to use shorter waveguide runs, the additional losses through rotary joints, T/R box, etc., will certainly produce an effect similar in magnitude to that estimated in Fig. 5 which shows 40 db loss at 1 mm, 12 db at 3 mm and 3.2 db at 1 cm.

The curve of peak transmitted power is quite realistic in the 1 to 10 cm range (0.25 to 4 megawatts) and perhaps slightly high at the extremely short and long wavelengths. The curves of minimum receiver sensitivities ($P_{\min}$) without maser amplifiers are also based upon measured values as reported by Dees and Sheppard (1963), and in the case of masers, as obtained by various workers in the field. Although masers have not yet been used at wavelengths of 1 cm or less, a parametric amplifier is available at 9 mm wavelength. Thus we have allowed the $P_{\min}$ curve with maser to run smoothly into the non-maser curve near 5 mm wavelengths.

Substituting the data of Fig. 5 into Eq. (20), we obtain the two curves of minimum detectable reflectivity as a function of wavelength shown in the upper half of the figure. Considering the decreasing transmitter powers available at millimeter wavelengths and the sharply increasing noise figures and RF losses, there is no escaping the fact that $\eta_{\min}$ must increase rapidly with decreasing wavelength below 1 cm. The only factor in favor of the shorter wavelengths is the increased beam filling effect and this is already as high as it can be at 1.36 cm.

5. Discussion

We have also plotted the two $\eta_{\min}$ curves of Fig. 5 in Fig. 4 for comparison with the reflectivity curves previously calculated as representative of CAT. It is immediately obvious from Fig. 4 that conventional radars of limited antenna size have no chance of detecting even the most reflective CAT at 18.5 km. Even with maser receivers and the most powerful transmitters, but limited antenna size, only the most reflective CAT ($C_n^2=10^{-14}$ cm$^{-\frac{2}{3}}$) is detectable, and then just barely. It is also abundantly clear that there is no point in considering wavelengths less than 1 or 2 cm since the $\eta_{\min}$ and η curves diverge extremely rapidly in the millimeter region.

In the hope that some improvement in overall system sensitivity would be attainable by integration techniques (or that we may have to employ large ground-based antennas), let us consider the required increase in sensitivity to detect moderately reflective CAT ($C_n^2=10^{-15}$ cm$^{-\frac{2}{3}}$). Since it is desirable to detect CAT of weak intensity, we take $\ell_m=1.0$ cm. We then calculate the ratio of $\eta_{CAT}/\eta_{\min}$ using the appropriate curves from Fig. 4 with the results shown in Fig. 6. Here it is obvious that the optimum wavelength is 8 cm where we require only a 9 db improvement in overall sensitivity. It is interesting, however, that the maximum of the curve is quite flat so that over the wavelength range of 4 to 100 cm, the required increase in sensitivity is less than 11 db. Thus, within this broad range of wavelengths, the choice can be based on other considerations such as size, weight, and other applications. Since components decrease in both size and weight with decreasing wavelength, and since the shorter wavelengths may also be used for cloud and storm detection with reasonably narrow beamwidths, a wavelength between 5 and 6 cm is quite obviously indicated.

While the choice of wavelengths is clear, it is to be emphasized that even the best airborne radar now feasible can barely detect the most reflective CAT ($C_n^2=10^{-14}$ cm$^{-\frac{2}{3}}$) and that a 20-db improvement is required to detect most CAT ($C_n^2\gtrsim 10^{-16}$). Such an improvement in an airborne system may just be attainable at the present state of the art using a coherent radar and prediction integration.

By way of comparison, we might also consider the use of large ground-based radars. The Wallops Island, Virginia, radars (3.2-, 10.7-, and 71-cm wavelengths with 34-, 60-, and 60-ft diameter antennas, respectively) used by Hardy *et al.* (1966) in probing the clear atmosphere are typical of such large state of the art systems. Their capability in detecting CAT of $C_n^2=10^{-15}$ cm$^{-\frac{2}{3}}$ at a range of 18.4 km is also indicated in Fig. 6. It is seen that both the 10.7- and 71-cm radars can detect such regions with a few decibels to spare. The use of maser amplifiers (instead of the parametric amplifiers now employed) and coherent integration should then bring most CAT within the range of detectability at modest ranges. Unfortunately, however, it does not appear economically feasible to install such major radars with the required density (about 30 miles apart) along the airways to provide reliable warnings. It would, however, be worth considering their use at points of common CAT occurrence.

Assuming that we may detect CAT regions (at least by large ground-based radars), the question arises as to how one may distinguish them from other non-CAT echoes. At the altitudes of interest cirrus clouds might well constitute a common false alarm. The reflectivity of typical cirrostratus is plotted as a function of wavelength in Fig. 4 based on the data of Plank *et al.* (1955) and unpublished data of the authors. Since the cloud particles are small, $\eta \propto \lambda^{-4}$. We see that the optimum airborne radar (with maser) can detect such clouds readily at all wavelengths shorter than about 15 cm. Accordingly, one might argue with some justification that a long wavelength is desirable in order to reduce

[6] L. F. O'Kelley: Radar frequency study including phase coherence. Unpublished report of Martin-Marietta Co., 30 June 1965.

[7] Sylvania Co., Microwave Diode Product Guide—91350761.

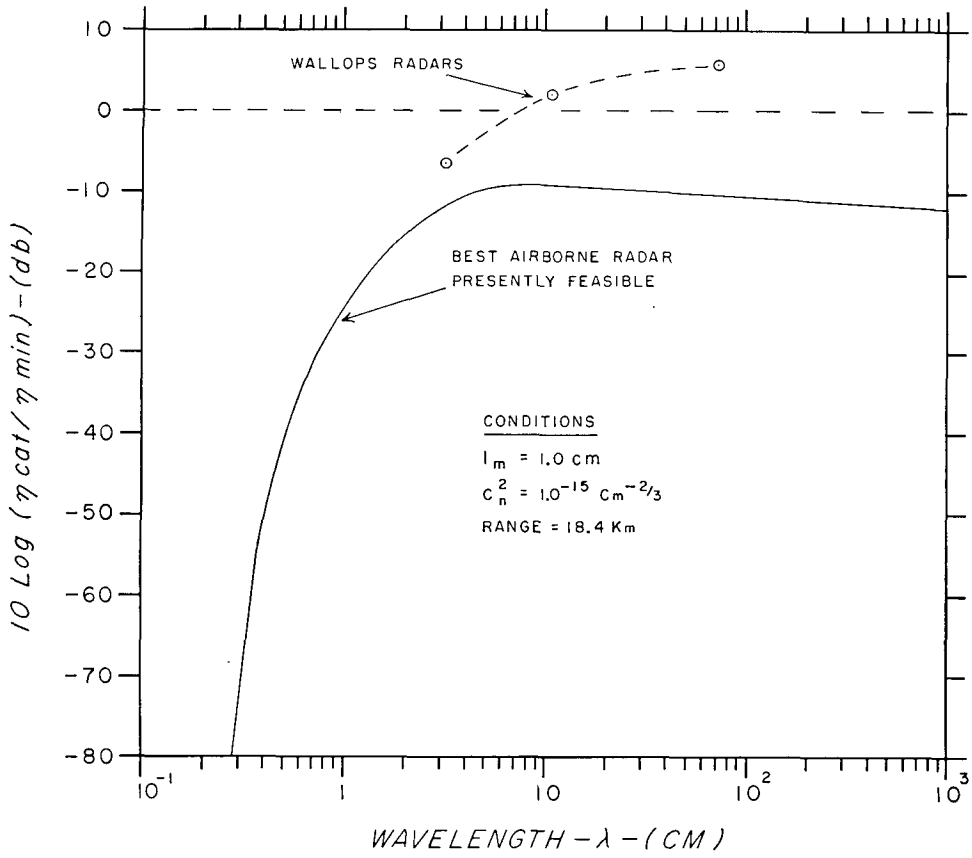

FIG. 6. Ratio of reflectivity expected from CAT (ℓ_m=1 cm, $C_n^2=10^{-15}$ cm$^{-\frac{2}{3}}$) to the minimum detectable reflectivity of the best airborne radar at 10 n mi range (solid curve). The present capability of the large radars at Wallops Island is also shown (dashed).

such false alarms. However, we shall soon see that cloud echoes may be a vital tracer for CAT detection.

In using the previously mentioned Wallops radars, Hardy *et al.* (1966) also commonly observed echoes from clear air layers of perturbed refractivity at altitudes up to about 5 km and occasionally higher. The reflectivities correspond to C_n^2 values up to about 10^{-14} cm$^{-\frac{2}{3}}$ and showed a wavelength dependence generally consistent with the $\lambda^{-\frac{1}{3}}$ law predicted in Fig. 4. However, the echo layers were invariably associated with sharp inversions of great thermal stability where the vertical gradient of refractivity M is very large. Thus, while the C_n^2 values [Eq. (15)] are large, and so too are the reflectivities, the mechanical turbulence is small. While the occurrence of such clear air echoes at CAT altitudes is much less common than lower down, it nevertheless points to the need for a means of measuring the intensity of mechanical turbulence within the various reflecting regions.

The general approach toward such a measurement has already been indicated by the work of Gorelik *et al.* (1963) and Rogers and Tripp (1964). The latter show that the total turbulent energy is directly proportional to the sum of the variance of the mean wind within the radar sampling volume and the mean variance of the turbulent wind within that volume. Both of these variances can be measured by means of a Doppler radar, while only the mean variance can be measured by conventional radar. However, if the turbulence spectrum is known, then the two variances are related and so only one needs to be measured. Gorelik *et al.* (1963) have already derived a relation between the variance of the echo fluctuation spectrum and ϵ which we have seen is a sensitive function of the turbulence intensity [Eq. (1b), Fig. 3]. The only assumption in such a relationship is that the scattering elements be reasonably good tracers of the turbulent wind. Such an assumption is undoubtedly valid for the ice crystals in cirrus clouds, and probably for chaff as well.

Since CAT regions are so difficult to detect directly and cirrostratus so readily detectable in the centimeter wavelength range (and indeed cirrus cloud frequently accompanies CAT), it is obvious that we should exploit the cloud echoes whenever they are present. Previously, we proposed a wavelength of 5 or 6 cm as the optimum for an airborne radar to detect CAT. With optimum radar characteristics, such a wavelength would provide a signal 18 to 20 db above noise for the typical cirrostratus cloud. Shorter wavelengths would

provide stronger cloud signals (Fig. 4), but would have little chance of detecting CAT directly in the absence of tracers. Thus, a wavelength of 5 to 6 cm is definitely indicated from both points of view.

In the absence of either direct CAT echoes or those from clouds, we might well consider the use of chaff. Properly selected slow-falling chaff dispersed either from aircraft or from the numerous radiosonde balloons released regularly, would provide measurable echoes for long periods of time without interfering with the longer wavelength ground-based radars.

Finally, a few words need to be said about the possible use of forward-scatter techniques. Calculations based upon Eq. (11) for a CAT region at 9 km height at the mid-point of a 10.7-cm scatter link having a 100-km base-line ($\theta/2=10.2°$) result in a reflectivity $\eta=58.5C_n^2$. Thus η_{CAT} ranges from about 6×10^{-15} to 6×10^{-13} cm^{-1} for C_n^2 from 10^{-16} to 10^{-14} cm$^{-\frac{2}{3}}$. [The great increase in forward-scatter reflectivity over that for back-scatter is due essentially to the $\sin^{-4}(\theta/2)$ dependence shown in Eq. (11).] Using 60-ft diameter antennas and the most sensitive receivers, it is readily shown that $\eta_{min}\sim4\times10^{-17}$ cm^{-1}. Thus, even the least reflective CAT should provide forward-scatter signals about 22 db above noise. Moreover, most of the region between the receiver and transmitter (and a swath a few miles wide to either side of the direct line of sight) could be kept under surveillance. Clearly, forward-scatter techniques hold great promise for reliable CAT detection.

6. Summary and conclusions

Previous theoretical work on the reflectivity of refractively turbulent media has been based on the spectrum of refractivity perturbations in the inertial subrange. In the present paper we derive an expression for the entire refractivity spectrum extending beyond the limiting microscale. This then permits the derivation of the reflectivity-wavelength dependence of the scattering from a turbulent medium for either back or bistatic scatter. For back scatter, the reflectivity is peaked at a wavelength $\lambda=5\ell_m$, where ℓ_m is the limiting microscale. Moreover, the previously predicted $\lambda^{-\frac{1}{3}}$ reflectivity-wavelength dependence is found to be valid only at $\lambda\gtrsim10\ell_m$.

The magnitude of the reflectivity of a turbulent medium depends upon the mean square fluctuation in refractivity or the coefficient C_n^2 in Tatarski's (1961) expression for the three-dimensional refractivity spectrum, and the reflectivity-wavelength variation is a function of ℓ_m at the shorter wavelengths. Reasonable ranges of both C_n^2 and ℓ_m are deduced for regions of CAT from theoretical considerations and empirical data. Based on these data, a tentative quantitative classification of CAT severity is proposed in terms of ϵ, the eddy energy dissipation rate, E_{100}, the turbulent energy at a scale of 100 m, ℓ_m, the limiting microscale, and σ_v, the rms turbulent velocity. Suggested thresholds of weak, moderate and severe CAT in terms of σ_v are roughly 0.67, 1.0 and 1.5 m sec^{-1}. The radar reflectivity of CAT regions is then calculated.

Using state of the art estimates of the optimum characteristics of radar, we compute the minimum reflectivity detectable by an airborne radar with a 1-m diameter antenna at a range of 10 n mi (1-min warning at 600-kt aircraft speeds) as a function of wavelength. The ratio of the reflectivity of a typical moderately reflective CAT region to the minimum detectable reflectivity is also calculated versus wavelength. It is found that the best state of the art airborne radars lack about 10 db of sensitivity to detect such CAT; a 20-db improvement in sensitivity is required to detect weakly reflective CAT regardless of its severity. Assuming that significant increases in sensitivity are attainable by integration techniques, or that ultra-sensitive ground-based radars are employed, the optimum wavelength is found to be about 5 to 6 cm. As wavelength is decreased below this optimum, the minimum detectable reflectivity increases sharply and the reflectivity of CAT decreases sharply. At wavelengths larger than the optimum, the ratio of CAT to minimum detectable reflectivity is virtually constant, and so the choice of wavelength can be based on considerations of size and weight of radar components. Since these are generally smallest at the shorter wavelengths, the wavelength region 5 to 6 cm is strongly indicated for implementation.

Since the optimum radar at 5 to 6 cm wavelength will also detect many clouds at a range of 10 n mi, the cloud echoes may be used as turbulence tracers by measuring either their Doppler or fluctuation spectra. Indeed, such measurements may be required in the case of clear air echoes as well if the reflectivity of CAT is not an indication of its severity (see Supplementary note).

Finally, calculations of the signals scattered in the near-forward direction by CAT regions show that they are considerably greater than those in the back-scatter direction and readily detectable by existing facilities. Forward-scatter techniques are thus suggested as a most promising means of reliable CAT detection.

7. Supplementary note

Within a few weeks following the completion of this paper, clear air echo layers were observed on several occasions by the 10.7- and 71-cm radars at Wallops Island in close correspondence to the height of the tropopause, and on one occasion at a height of 8 km in a layer of light CAT. In one case which has been analyzed, the tropopause echoes corresponded to $C_n^2=10^{-15}$ cm$^{-\frac{2}{3}}$ and agreed with the $\lambda^{-\frac{1}{3}}$ reflectivity-wavelength dependence.[8] Thus this early confirmation of our estimate of C_n^2 at high altitudes is gratifying.

[8] Atlas, D., K. R. Hardy, K. M. Glover, I. Katz and J. G. Konrad, 1966: Radar observation of the tropopause. To be submitted for publication.

Using values of the vertical refractivity gradient and wind shear at the height of the echo layer, we computed $L_0 = 70$ m, $\epsilon = 390$ cm^2 sec^{-3} and $R = 4.7$ cm$^{\frac{3}{2}}$ sec^{-1}. Thus, the region must have been in the category of moderate turbulence in our scale (Table 1) or heavy in that of MacCready *et al.* (1965). The indications are that a value of C_n^2 of 10^{-15} cm$^{-\frac{2}{3}}$ at 12 km can occur only with an outer scale L_0 which, in association with average shear at the tropopause, implies at least light turbulence. Thus, simple detection of high altitude layers by the Wallops Island radars is indicative of some degree of mechanical turbulence. However, the absence of echoes is not a sign of non-turbulent conditions.

REFERENCES

Atlas, D., 1964: Advances in radar meteorology. *Adv. in Geophys.*, **10**, 317–478.

Dees, J. W., and A. P. Sheppard, 1963: Components, performance and cost of MM-wave systems. *Microwaves*, July, 18–27.

Gorelik, A. G., 1965: Atmospheric turbulence research by radar methods. *Moscow.**

——, I. U. V. Mel'nichuk and A. A. Chernikov, 1963: The statistical characteristics of the radar echo as a function of the dynamic processes and microstructure of the meteorological entity. *Moscow. Tsentral'naia Aerologicheskaia Observatoriia, Trudy*, No. 48, 3–54. English translation T-R-479, Air Force Cambridge Research Laboratories, Bedford, Mass., 91 pp.

Gurvitch, A. S., L. R. Tsvang and A. M. Yaglom, 1965: Empirical data on the small-scale structure of atmosphere turbulence. *Moscow.**

Hardy, K. R., D. Atlas and K. M. Glover, 1966: Multi-wavelength backscatter from the clear atmosphere. *J. Geophys. Res.*, **71**, 1537–1552.

* The papers indicated by *Moscow* were presented at the International Colloquium on the Fine-Scale Structure of the Atmosphere, URSI-UGGI, Moscow in June 1965. A conference proceedings is being prepared for publication by the Institute of Atmospheric Physics, Moscow.

MacCready, P. B Jr., 1962: The inertial subrange of atmospheric turbulence. *J. Geophys. Res.*, **67**, 1051–1059.

——, R. E. Williamson, S. Berman and A. Webster, 1965: Operational application of a universal turbulence measuring system. Contractor report NASA CR-62025 by Meteorology Research, Inc., Altadena, Calif., 12 pp., 5 appendices. Available from NASA.

Megaw, E. C. S., 1957: Fundamental radio scatter propagation theory. *Proc. IEE.* **104C**, 441–455.

Nichols, L., R. Edwards and H. J. Krahn, 1964: Millimeter-wave generators. *Electro-Technology*, **74**, 63–84.

Obukhov, A. M., 1949: Local structure of atmospheric turbulence. *Izvest. Akad. Nauk SSSR Ser. Geofiz.*, **13**, 58.

Panofsky, H. A., 1965: The fine-scale structure of the atmosphere above the surface layer in clear air. *Moscow.**

——, and F. Pasquill, 1963: The constant of the Kolmogorov law. *Quart. J. R. Meteor. Soc.*, **89**, 550–551.

Pao, Y. H., 1964: Distribution of turbulent energy and concentrations at large wave numbers. Boeing Flight Sciences Lab. Rpt. No. 90, Seattle, Wash., 77 pp. Available from Boeing Scientific Research Laboratories.

Plank, V. G., D. Atlas and W. H. Paulsen, 1955: The nature and detectability of clouds and precipitation as determined by 1.25 centimeter radar. *J. Meteor.*, **12**, 358–378.

Reiter, E. R., and A. Burns, 1965: Atmospheric structure and clear-air turbulence. *Moscow.**

Rogers, R. R., and B. R. Tripp, 1964: Some radar measurements of turbulence in snow. *J. Appl. Meteor.*, **3**, 603–610.

Smith, P. L., and R. R. Rogers, 1963: On the possibility of radar detection of clear-air turbulence. *Proc. Tenth Weather Radar Conf.*, Boston, Amer. Meteor. Soc., 316–322.

Tatarski, V. I., 1960: Radiophysical methods for the investigation of atmospheric turbulence. *Radiofizika*, **3**, No. 4, 551–583.

——, 1961: *Wave Propagation in a Turbulent Medium*. New York, McGraw-Hill Book Co., 285 pp.

——, 1965: Line-of-sight propagation fluctuations. *Moscow.**

Vinnichenko, N. K., N. Z. Pinus and G. N. Shur, 1965: Some results of the experimental turbulence investigations in the troposphere. *Moscow.**

Wilkins, E. M., 1963: Decay rates for turbulent energy throughout the atmosphere. *J. Atmos. Sci.*, **20**, 473–476.